a) For problems of the $2m$th order the condition number $Cn(K)$ of K varies as h^{-2m} or as Ne^{2m}, where Nes denotes the number of elements per side.

b) The condition number depends primarily on the nature of the problem and not on the order of the finite element. Therefore, it is expected that by using high-order elements greater total accuracy would be achieved in the finite element solution. This will be demonstrated numerically in the next section.

Numerical experiments

Higher order elements were applied to a beam problem to test the possibility of a reduction of the relative effect of roundoff error accumulation in the solution of the global system of algebraic equations. For comparison, two elements were used. One was denoted by $B(3)$, since the lateral deflection w was interpolated inside it by cubic polynomials ($p = 3$). The other was denoted by $B(5)$, since inside it w was interpolated by quintic polynomials ($p = 5$). From the numerical calculations it follows that the condition number can be expressed by $Cn(K) = 8Ne^4$ in the case where $B(3)$ elements were used and by $Cn(K) = 15Ne^4$ in the case where $B(5)$ elements were used. In any case the condition number varies only slightly with p.

To study the behavior of roundoff error effects for matrices generated by the $B(3)$ and $B(5)$ elements, the displacement of a cantilever beam loaded at the tip by a single force was calculated using Gauss elimination in single (24 bits, $s = 7.2$) precision. Both with $B(3)$ and $B(5)$ elements there are no discretization errors, the sole errors being numerical. It has been found that the error δx_t in the tip deflection x_t (this error is proportional to the error in the energy) can be expressed by

$$\log(\delta x_t/x_t) = -7.53 + 1.16 \log(Cn) \qquad (10)$$

when the $B(3)$ element was used and by

$$\log(\delta x_t/x_t) = -8.01 + 1.16 \log(Cn) \qquad (11)$$

when the $B(5)$ element was used. This is remarkably close to estimate (5).

The fact that by using higher order elements one may be able to achieve greater accuracy is confirmed in Fig. 1. It shows the variation of the relative total error in the energy vs the number of degrees of freedom N for the case of a cantilever beam loaded by a quadratically varying load. Computation was carried out in single precision. Even though roundoff errors become dominant earlier with the $B(5)$ element (at $N = 12$) than with the $B(3)$ element (at $N = 22$), it was possible to obtain a greater total accuracy with the former element than with the latter.

These were one-dimensional experiments. The precise manner in which both c in $Cn(K) = ch^{-2m}$ and the roundoff errors depend on the dimension in higher dimensional problems is still to be determined.

References

[1] Fried, I., "Discretization and Round-Off Errors in the Finite Element Analysis of Elliptic Boundary Value and Eigenvalue Problems," Ph.D. thesis, May 1971, Dept. of Aeronautics and Astronautics, MIT.

[2] Bauer, F. L., "Optimal Scaling and the Importance of the Minimal Condition," *Information Processing 1962*, edited by C. M. Popplewell, North-Holland Publishing, Amsterdam, 1963, pp. 198–200.

[3] Melosh, R. J. and Palacol, E. L., "Manipulation Errors in Finite Element Analysis of Structures," CR-1385, Aug. 1969, NASA.

[4] Fitzgerald, B. K. E., "Error Estimates for the Solution of Linear Algebraic Systems," *Journal of Research*, National Bureau of Standards-B. Mathematical Sciences, Vol. 74B, Oct.-Dec. 1970, pp. 251–310.

[5] Kelsey, S., Lee, K. N., and Mak, C. K. K., "The Condition of Some Finite Element Coefficient Matrices," *Computer-Aided Engineering, Proceedings of the Symposium held at the University of Waterloo, Canada*, May 11–13, 1971, edited by G. M. L. Gladwell, pp. 267–283.

[6] Sluis, A. Van der, "Condition Equilibration and Pivoting in Linear Algebraic Systems," *Numerische Mathematik*, Vol. 15, 1970, pp. 74–86.

[7] Fox, L. R. and Stanton, E. L., "Development in Structural Analysis by Direct Energy Minimization," *AIAA Journal*, Vol. 6, No. 6, June 1968, pp. 1036–1042.

Calculation of a Slender Body Moving through Air at Supersonic and Subsonic Velocities

M. L. WILKINS*

University of California, Lawrence Radiation Laboratory, Livermore, Calif.

THE finite difference solutions of the equations of gas dynamics formulated in Lagrange coordinates are capable of accuracies of 1 part in 10^3 for problems with a reasonable number of Lagrange zones. Finite difference techniques permit physical phenomena to be simulated in a time-dependent manner, starting from actual initial conditions. Also, there are no restrictions on models used to describe the behavior of materials. The main strengths of the Lagrange formulation are the ease of applying boundary conditions and high accuracy. The major limitation of the Lagrange formulation is that nearest neighbors of the Lagrange zones must remain nearest neighbors, except for specified lines of sliding.

In the calculations presented here, a slender body of revolution defined by a set of Lagrange coordinates moves into another set of Lagrange points that have associated with them an equation of state appropriate for air. The specified line of sliding is the set of Lagrange coordinates that define the exterior boundary of the figure of revolution.

The slender body moving in the air, which is initially at rest, is shown in Fig. 1. The equation of state used for air is described by a perfect gas, although any equation of state could be used. The velocity of the slender body is given in units of the sound speed of the undisturbed air ahead of the body (Mach number). The shocks develop automatically in the calculation by the artificial viscosity method originated by Von Neumann and Richtmyer.[1] The shock positions shown in Fig. 1 are plotted by a computer routine that scans the grid and plots a symbol at positions where the artificial viscosity is a maximun. A steady-state shock pattern is established after the body has completely entered the calculation region (Fig. 1b). A steady-state shock pattern means that shock angles with respect to the body remain constant in time although the shocks are sweeping through new material. At time $t = 200$ μsec, the body is programed to reduce velocity on a linear ramp with time. The shock angles are shown, in Fig. 1, c–f, to open as the velocity is reduced. The bow shock detaches when the velocity becomes subsonic (Fig. 1, d–f).

To a fixed observer, the bow and aft shocks are moving faster than the slender body for the subsonic velocities shown in Fig. 1, e and f. At $t = 800$ μsec the body is programed to increase velocity on a linear ramp with time (Fig. 1, g and h). New bow and aft shocks are formed. Figure 1g shows

Received April 12, 1971; revision received June 3, 1971. This work was performed under the auspices of the U.S. Atomic Energy Commission.

Index category: Subsonic and Transonic Flow.

* Physicist.

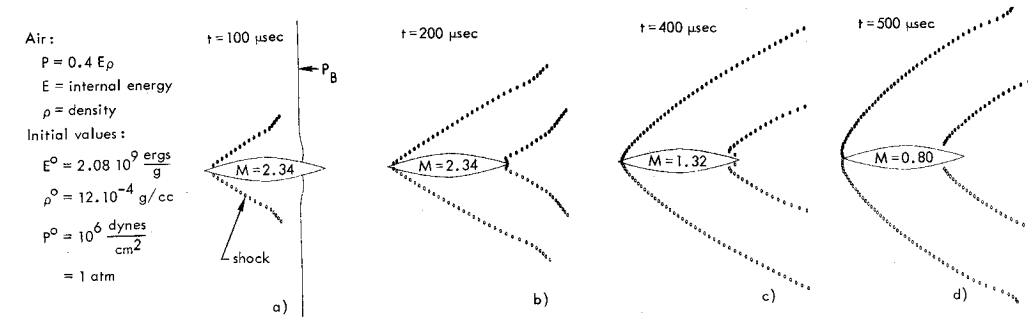

Fig. 1 Calculation of a slender body with cylindrical symmetry moving, through air at rest, at supersonic to subsonic velocity. a) The slender body enters region of calculation from right. P_B = boundary. pressure = 1 atm. b) Steady-state shock pattern. c) Bow shock angle opens as slender body slows to lower Mach number. d) Subsonic velocity; bow shock starts to detach.

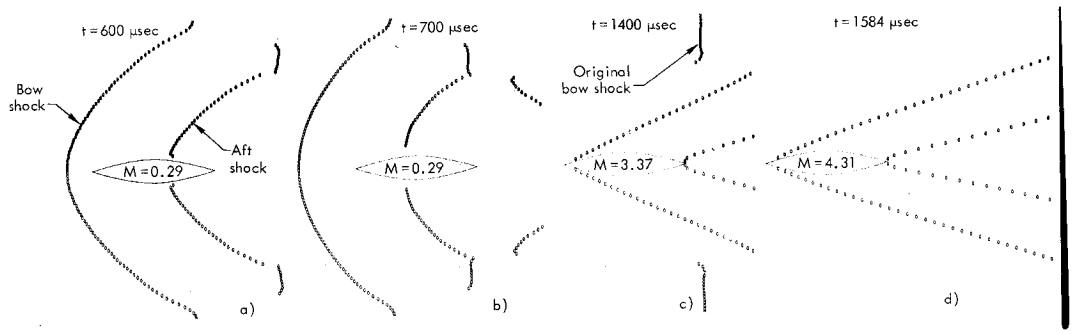

Fig. 2 Calculation of a slender body with cylindrical symmetry moving through air at subsonic to supersonic velocity. Conditions are as shown in Fig. 1. a) Bow shock completely detached from slender body; aft shock moves forward. b) Aft shock continues to move forward. Extra shocks are reflections of bow and aft shocks from top and bottom rigid boundaries. c) Slender body programed to higher velocities, overtakes, breaks through original bow shock. d) Shock angles decrease as higher Mach numbers are reached.

the new bow shock breaking through the original bow shock that was ahead of the slender body.

The direction of the motion of each of the Lagrange grid points is shown in Fig. 2a at time $t = 250$ μsec. It is noted that the bow shock is due to the compression of the quiet air by the motion of the slender body. A decompression or rarefaction is seen emanating from the high portion of the body as the air moves in opposite directions. The aft shock is seen to be produced by air which is being compressed by air moving into the same position from opposite directions.

Figure 2b shows contours of equal pressure for the same time as Fig. 2a. The Lagrange grid used in the calculation is shown in Fig. 2c. All of the plots in Figs. 1 and 2 were obtained automatically by the computer as the problem progressed.

Because of the cylindrical symmetry, only one half of the problem need be calculated. The remaining half is obtained by reflection about the axis of symmetry as in Fig. 2c. Thirty-five grid points were used in the radial direction. In the axial direction, grid points were added in front of and removed from behind the body as time progressed to minimize the computation time without affecting the results in the area of interest.

The calculation was done with the HEMP[2] code on an IBM 7030 computer. The computer time was $2\frac{1}{2}$ hr. The code is currently operating on a CDC 7600 computer with a speed increase factor of 10. Programing is in process for the CDC STAR computer, where an additional speed increase factor of 15 is expected. A three-dimensional version of the code (three independent Cartesian coordinates and

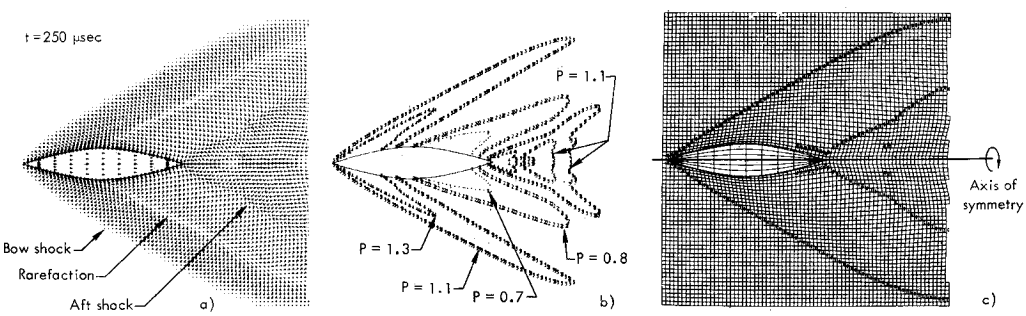

Fig. 3 Details of the flow of time $t = 250$ μsec when the Mach number is 2.0. a) Small arrows show direction of material velocity. b) Contours of constant pressure P in atmospheres. c) Shock positions and Lagrange calculational grid.

time) is in operation on the CDC 7600.[3] A three-dimensional calculation with the same detail as the two-dimensional calculation presented here would require 35 times the number of zones and four quadrants instead of one. The total number of zones required would be 140 times the number used and the computer time would increase by the same factor. By replacing the IBM 7030 with the STAR computer, a 150 fold increase in computation speed is achieved. This more than offsets the increase in computation time required for a similar three-dimensional calculation. Thus, with the STAR computer, it will be possible to simulate the general three-dimensional problem of a body moving through air at a finite angle of attack in the same computer time as the two dimensional problem given here.

References

[1] Von Neumann, J. and Richtmyer, R. D., "A Method for the Numerical Calculation of Hydrodynamic Shocks," *Journal of Applied Physics*, Vol. 21, No. 3, March 1950, pp. 232–237.

[2] Wilkins, M. L., "Calculation of Elastic Plastic Flow," UCRL-7322 Rev. I, Jan. 24, 1969, Lawrence Radiation Lab., Livermore, Calif.

[3] Wilkins, M. L., French, S. J., and Sorem, M., "Finite Difference Scheme for Calculating Problems in Three Space Dimensions and Time," UCRL-72634, Aug. 13, 1970, Lawrence Radiation Lab., Livermore, Calif.

Exact Numerical Solutions for Transient Shear Stress and Boundary-Layer Induced Pressure

Czeslaw M. Rodkiewicz*
University of Alberta, Edmonton, Canada

AND

Roop N. Gupta†
NASA Langley Research Center, Hampton, Va.

Nomenclature

C = $\mu\rho/\mu_\infty\rho_\infty$
f = function related to the stream function by $\psi = [2\nu_\infty CtU_\infty]^{1/2} f(\eta,\xi)$
Δf = $f - f_2$
h = local enthalpy
H = total enthalpy, $= h + u^2/2$
I = $\int_0^\infty \left\{ S_w + \frac{[(\gamma-1)/2]M_\infty^2}{(1+[(\gamma-1)/2]M_\infty^2)} f' \right\} (1-f')d\eta$
J = $\int_0^\infty [1-f']d\eta$
M_∞ = freestream Mach number
Pr = Prandtl number
p = Static pressure
Δp = $p_{w,2} - p_w$
Re_{x_∞} = $\rho_\infty U_\infty x/\mu_\infty$
S = total enthalpy ratio, $= H/H_\infty$
t = time
u = x-component of velocity
U = plate velocity
ΔU = impulsive change in plate velocity, $= (U_2 - U_1)_\infty$
x,y = coordinates along and normal to the plate, respectively
γ = ratio of specific heats
δ_ρ = density defect thickness, $\int_0^\infty \left(1 - \frac{\rho}{\rho_\infty}\right) dy$
δ^* = mass flow defect thickness, $\int_0^\infty \left[1 - \frac{\rho u}{(\rho U)_\infty}\right] dy$
ξ = similarity independent variable associated with time and space, $= (U_\infty t/x)/(U_\infty t/x) + 1$
η = similarity independent variable associated with space, $= \left[\frac{U_\infty}{2\nu_\infty Cx}\right]^{1/2} \int_0^y \frac{\rho}{\rho_\infty} dy$
μ = dynamic viscosity
ν = kinematic viscosity
ρ = density
χ = hypersonic interaction parameter, $M_\infty^3/(Re_{x_\infty}/C)^{1/2}$
ψ = stream function
τ = $U_\infty t/x$

Subscripts

∞ = freestream value
w = quantity at the plate surface
1 = initial steady state
2 = final steady state

Superscripts

$'$ = differentiation with respect to η

A FIRST order perturbation solution for the temporal weak-interaction induced pressure was obtained in Refs. 1 and 2 for the case of a flat plate moving at hypersonic speed and subjected to an impulsive velocity increment of 1%. Whereas these solutions seem adequate for the calculation of the transient contribution to the induced pressure, this does not appear to be true for the estimation of the time-dependent component of the wall shear. The basic linearizing assumption of $\Delta f \ll f_2$, contained in Ref. 2, breaks down near $\tau = 0$ even when the fractional change in the plate velocity is small. The purpose of this Note is to report on a numerical solution to this problem without the use of a linearization procedure so that problems involving the accurate prediction of wall shear for plate velocity changes of 1% or larger may be treated.

The time-dependent boundary-layer equations, for zero pressure gradient and $Pr = 1$, in the transformed η, ξ plane are

$$2(1-\xi)^2 \frac{\partial f}{\partial \xi} - 2\xi(1-\xi)\left(f' \frac{\partial f'}{\partial \xi} - \frac{\partial f}{\partial \xi} f''\right) - ff'' - f''' = 0 \quad (1)$$

$$2(1-\xi)^2 \frac{\partial S}{\partial \xi}\left[1 - \frac{\xi f'}{(1-\xi)}\right] - S'' - S'\left[f - 2\xi(1-\xi)\frac{\partial f}{\partial \xi}\right] = 0 \quad (2)$$

(The coordinate system chosen is fixed with reference to the plate and its origin is at the leading edge.)

Equations (1) and (2) are similar to those given in Ref. 2 (before introduction of the assumption $\Delta f \ll f_2$), except for the definitions of the independent variable ξ and the dependent variable S. The solution of the momentum Eq. (1) is obtained by a numerical method.[3] Once the f' distribution is known, the S distribution may be obtained from

$$S(\eta,\xi) = f'(\eta,\xi) + S_w\{1 - f'(\eta,\xi)\} \quad (3)$$

which satisfies Eq. (2) and the relevant boundary conditions.

The numerical method, used here, is based on the Clutter-Smith technique[3] which solves the time-steady compressible laminar boundary-layer equations in two independent variables. This is an implicit finite-difference technique that is known to produce accurate results and has been well explored. In this method of solution the derivatives with respect to ξ (analogous to the spatial variable of Ref. 3 in the streamwise direction) are replaced by their finite-difference

Received April 12, 1971; revision received June 14, 1971. The authors would like to acknowledge the useful comments made by I. E. Beckwith during the preparation of the final manuscript.

Index category: Supersonic and Hypersonic Flow.

* Associate Professor, Mechanical Engineering.

† National Academy of Science Research Associate, Hypersonic Vehicles Division.